the method used in this study, we measured the toluene second ionization energy, and the value obtained was 15.2 eV which is 0.5 eV lower than the value 15.7 eV extracted from the ionization efficiency curve of doubly charged toluene.[65]

The peak shape of the doubly charged fullerene ions reveals a strong tail to lower energy, especially when compared to that for toluene (see Figure 14). The shape of the $C_{60}^{2+}$ charge-stripping peak for $O_2$ resembles those of the other collision gases. This degree of tailing is not commonly observed in charge-stripping peaks of smaller organic cations.[37,38] There are two probable explanations. The ion population of the low-energy tail consists of those ions that have lost additional kinetic energy by transfer of momentum to the $O_2$ collision gas, analogous to the results discussed for He, implying that nearly direct collisions are occurring in the charge-stripping process. Alternatively, the ion population of the low-energy tail consists of those doubly charged ions that have converted some kinetic energy, in addition to that used to remove the electron, into internal energy of the doubly charged ion. One mechanism for exciting the doubly charged ion is by removal of low-lying electrons, which may be a facile process owing to the unusual electronic structure of the fullerenes. Doubly charged ions that form in a collision to give internally excited target gas would also appear in the low-energy tail.

## Conclusion and Summary

Both a three-sector and a four-sector mass spectrometer were used to study the products of high-energy collisions of fullerene molecular ions with various target gases. Small target gases are captured directly, and the various endohedral complexes are observed as product ions. Evidence for capture of Ar is indirect owing to the high internal energy of the Ar endohedral complex formed by high-energy collisions. Analysis of the kinetic energies of the product ions produced from He and $D_2$ collisions leads to the conclusion that the endohedral complex fragments to produce the observed product ions. Charge stripping of the fullerene precursor ions leads to the production of abundant doubly charged molecular ions, and this allowed the apparent second ionization energy of $C_{60}$, $C_{70}$, and $C_{84}$ to be measured.

Reasonable conclusions can now be drawn about mechanistic details. For example, the direct loss of an intact $C_{10}$ unit from $C_{70}He^{\cdot+}$ to produce $C_{60}He^{\cdot+}$ should open a hole in the carbon cage and allow the He atom to escape. If the $C_{60}He^{\cdot+}$ species, however, were formed by consecutive $C_2$ losses from $C_{70}He^{\cdot+}$, then the carbon cage could anneal, preventing He escape.

For $C_{60}He^{\cdot+}$, the end point of $C_n$ loss is $C_{44}He^{\cdot+}$. It is difficult to accept that the direct loss of a $C_{16}$ molecule would not allow release of the entrapped He. The bond lengths for $C_{60}$ are 1.4 and 1.45 Å,[21] which are approximately half the van der Waals diameter of He, in line with this simple argument for consecutive $C_2$ loss from $C_{60}He^{\cdot+}$. Unpublished results of a theoretical calculation[66] also support a consecutive $C_2$ loss mechanism.

High-energy collisional activation and MS/MS should prove to be an effective tool for qualitative analysis of other fullerenes, fullerene analogues, and fullerene-based materials. A test for the presence of a closed-cage structure is capture of a He atom or other noble gas atoms. If the product ions containing He are considered interferences, then $N_2$ or $O_2$ should be used as a collision gas.

**Acknowledgment.** We are grateful to Robert Bateman of VG Analytical (Fisons Instruments) who designed the four-sector tandem mass spectrometer used in this work and who advised us on experimental aspects of this work. K.A.C. expresses sincere appreciation to Don Rempel for the informative late-night chalkboard discussions of electrostatic analyzers and their aberrations, and the energetics associated with various fragmentation pathways. The research was supported by the National Science Foundation (Grant No. CHE 9017250).

(65) Dorman, F. H.; Morrison, J. D. *J. Chem. Phys.* **1961**, *35*, 575.

(66) Reference 13 in ref 42 of this paper.

# Solid-State Reactions Studied by Carbon-13 Rotor-Synchronized Magic Angle Spinning Two-Dimensional Exchange NMR. 1. Self-Diffusion and the Tautomeric Hydrogen Shift in Tropolone

**Jeremy J. Titman, Zeev Luz,† and Hans W. Spiess***

*Contribution from the Max-Planck-Institut für Polymerforschung, Postfach 3148, D-6500 Mainz, Germany.* *Received November 12, 1991*

**Abstract:** Two-dimensional carbon-13 magic angle spinning exchange NMR experiments with rotor-synchronized mixing times have been carried out for solid tropolone at 40 °C and at variable spinning frequencies. At low spinning rates, a complicated spectrum is obtained with cross peaks linking different sidebands of the same carbon atom ("auto" cross peaks) as well as ones linking sidebands of chemically different atoms that are exchanged by a tautomeric hydrogen shift process ("hetero" cross peaks). The results are interpreted in terms of a translational diffusion mechanism in which tropolone molecules undergo lattice jumps between different sites. To retain the crystal order, certain lattice jumps require that the molecules undergo a concomitant hydrogen shift and/or a $\pi$-flip about an axis in the molecular plane. From the results, a self-diffusion constant of $D \simeq 4 \times 10^{-21}$ m$^2$ s$^{-1}$ is estimated for solid tropolone at room temperature.

## Introduction

Tropolone is one of a family of $\alpha$-hydroxy ketones which undergo a tautomeric hydrogen shift reaction. In solution the proton and carbon-13 NMR spectra always exhibit averaged signals due to the two tautomeric forms from which a lower limit of $10^8$ s$^{-1}$ can be set for the rate of the hydrogen shift at room temperature.[1,2]


† Permanent address: The Weizmann Institute of Science, Rehovot 76100, Israel.

0002-7863/92/1514-3756$03.00/0 

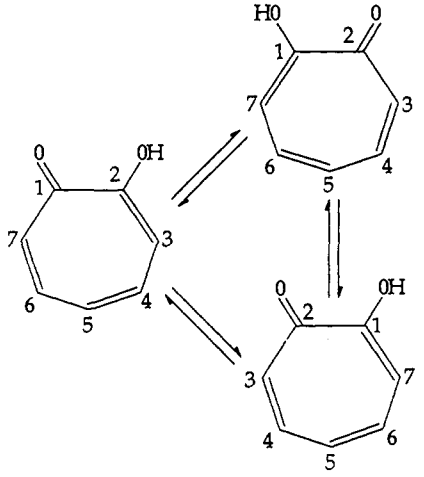

**Figure 1.** Schematic diagram showing pure hydrogen shift in solid tropolone (top left side of triangle) and a concerted hydrogen shift/molecular $\pi$-flip (bottom left side of triangle). The right side shows a pure molecular $\pi$-flip following the hydrogen shift; the combination of these makes the concerted process. The numbers in the left structure give the numbering convention used in the present work. The numbers on the other structures show the sites at which the various carbon atoms end up at the different stages of the dynamic process.

The activation energy for hydrogen transfer between the two degenerate forms of tropolone in solution is apparently low, no restrictions being imposed on the reaction by the surrounding solvent molecules.[3,4] In contrast, in solid tropolone the rate of this process is extremely slow. A neutron scattering study using a high-resolution beam revealed no effects associated with quantum mechanical tunneling of the hydroxyl hydrogen atom in either tropolone or tropolone-$d_1$.[5] One- and two-dimensional carbon-13 magic angle spinning (MAS) NMR experiments have indicated that the half-life of the hydrogen shift reaction at room temperature is about 10 s with an activation energy[6,7] of ~26 kcal mol$^{-1}$. Such a dramatic decrease in the rate of intramolecular chemical reactions in solids with respect to liquids is often encountered and the phenomenon has been termed the kinetic solid-state effect (KSSE).[8] It has been argued[7] that the high activation energy for the tautomeric hydrogen shift in solid tropolone stems from the fact that the reaction is associated with a concomitant $\pi$-flip of the molecules, which restores them to their original orientation in the crystal lattice (Figure 1). This reasoning makes use of crystallographic X-ray studies[9] of tropolone, which have shown that the crystals are highly ordered with the molecules forming coplanar hydrogen-bonded pairs. If a hydrogen shift were to take place without a concomitant $\pi$-flip, a disordered structure would be obtained. While on these grounds the concerted mechanism seems very sound, the NMR study referred to above does not provide firm evidence for its occurrence since it was carried out with a spinning rate, $\omega_R$, fast compared to the width of the chemical shift anisotropy, $\omega_L\Delta\sigma$. Under this condition, the anisotropic part of the chemical shift interaction and, thus, any information about reorientation processes are lost. In the present work, we investigate this system using a modified two-dimensional MAS exchange experiment[10-12] employing a rotor-synchronized mixing time. This experiment is carried out at low spinning rates compared with the width of the chemical shift anisotropy and can, therefore, detect pure molecular reorientation processes as well as chemical exchange or, indeed, a concerted combination of the two.

A related study is that of Haeberlen and co-workers.[13] These authors noticed that hydrogen transfer within hydrogen-bonded carboxylic acid dimers in solids is sometimes associated with anomalously high activation energies of ~15 kcal mol$^{-1}$ compared to the more common range of between 1 and 2 kcal mol$^{-1}$. They proposed that, in the systems exhibiting high activation energies, the process involves a flip of the whole dimeric unit followed by rapid hydrogen transfer. Using proton, deuterium, and carbon-13 NMR of single crystals, they were able to prove this mechanism in solid dimethylmalonic acid. Similar situations may be encountered in some of the organic bases studied by Limbach and co-workers.[14]

Two-dimensional NMR exchange spectroscopy has proved extremely useful in studies of chemical reactions in solutions, in particular, for spin-$^1/_2$ nuclei such as proton and carbon-13[15,16] for reactions that are slow compared to the transverse relaxation rate but still fast compared to the longitudinal relaxation rate. This regime is sometimes referred to as the "ultraslow" regime. The two-dimensional spectra obtained in such experiments show peaks along the main diagonal at positions corresponding to the normal resonance frequencies as well as cross peaks linking the signals of exchanging atoms. As mentioned above, the technique has also been applied to carbon-13 MAS NMR of fast spinning samples.[6] Under these conditions, the two-dimensional spectra are essentially identical with those in liquids. At low spinning frequencies ($\omega_R < \omega_L\Delta\sigma$), however, a two-dimensional pattern can be obtained from which information about reorientation processes can be retrieved. It should be noted that applying the standard two-dimensional experiment in these circumstances leads to cross peaks linking different sidebands of the individual carbon resonances even in the absence of a molecular reorientation. This is because the orientation of a particular crystallite in the powder with respect to the static magnetic field and, therefore, also the chemical shift of a given carbon atom at the beginning and at the end of an arbitrary mixing period will in general be different. This results in a set of cross peaks similar to that observed for a real molecular reorientation. If, however, as suggested by Veeman and co-workers,[10,11] the mixing time is set equal to an integral number of rotor periods

$$\tau_m = N2\pi/\omega_R = NT_R$$

a given crystallite always has the same orientation at the beginning as at the end of the mixing period. Thus, no cross peaks appear unless a real reorientation took place. A quantitative analysis of the relative intensities of the cross peaks can, in principle, provide information about the geometry and the rate of the reorientation process.

This form of the experiment does not allow recording of pure absorptive line shapes resulting in loss of resolution and the spectra are usually displayed in the magnitude mode. A solution to this difficulty has recently been proposed by Hagemeyer et al.[12] who

(1) Weiler, L. *Can. J. Chem.* **1972**, *50*, 1975.
(2) Bertelli, D. J.; Andrews, T. G., Jr.; Crews, P. O. *J. Am. Chem. Soc.* **1969**, *91*, 5286.
(3) Jackman, L. M.; Trevella, J. C.; Haddon, R. C. *J. Am. Chem. Soc.* **1980**, *102*, 2519.
(4) Rios, M. A.; Rodriguez, J. *Can. J. Chem.* **1991**, *69*, 201.
(5) White, J. W. *Spectrochim. Acta* **1981**, *A37*, 1041.
(6) Szeverenyi, N. M.; Sullivan, M. J.; Maciel, G. E. *J. Magn. Reson.* **1982**, *47*, 462.
(7) Szeverenyi, N. M.; Bax, A.; Maciel, G. E. *J. Am. Chem. Soc.* **1983**, *105*, 2579.
(8) Limbach, H. H.; Hening, J.; Kendrick, R.; Yannoni, C. S. *J. Am. Chem. Soc.* **1984**, *106*, 4059.
(9) Shimanouchi, H.; Sasada, Y. *Acta Crystallogr.* **1973**, *B29*, 81.
(10) (a) de Jong, A. F.; Kentgens, A. P. M.; Veeman, W. S. *Chem. Phys. Lett.* **1984**, *109*, 337. (b) Kentgens, A. P. M.; de Jong, A. F.; de Boer, E.; Veeman, W. S. *Macromolecules* **1985**, *18*, 1045.
(11) Kentgens, A. P. M.; de Boer, E.; Veeman, W. S. *J. Chem. Phys.* **1987**, *87*, 6859.
(12) Hagemeyer, A.; Schmidt-Rohr, K.; Spiess, H. W. *Adv. Magn. Reson.* **1989**, *13*, 85.
(13) Scheubel, W.; Zimmermann, H.; Haeberlen, U. *J. Magn. Reson.* **1988**, *80*, 401.
(14) Smith, J. A. S.; Wehrle, B.; Aguilar-Parrilla, F.; Limbach, H. H.; de la Concepcion Foces-Foces, M.; Cano, F. H.; Elguero, J.; Baldy, A.; Pierrot, M.; Khurshid, M. M. T.; Larcombe-McDouall, J. B. *J. Am. Chem. Soc.* **1989**, *111*, 7304.
(15) Ernst, R. R.; Bodenhausen, G.; Wokaun, A. *Principles of Nuclear Magnetic Resonance in One and Two Dimensions*; Clarendon Press: Oxford, 1987; Chapter 9.
(16) Perrin, C. L.; Dwyer, T. J. *Chem. Rev.* **1990**, *90*, 935.

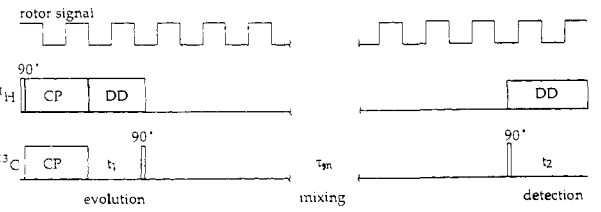


**Figure 2.** Pulse sequence used for the carbon-13 CPMAS rotor-synchronized two-dimensional exchange experiments. An optical signal reflected from the rotor triggers the cross polarization, which is followed by an incremented evolution period $t_1$ and then a $\pi/2$ pulse. After an approximately preset mixing time, a second optical signal initializes an additional delay (set equal to the cross-polarization period plus the evolution period for the normal experiment or to just the cross-polarization period for the time-reversed experiment) after which the mixing period is terminated by the detection pulse. This procedure ensures that the mixing times are $NT_R$ and $NT_R - t_1$ respectively for the normal and time-reversed experiments.

combined Veeman's experiment with a "time-reversed" version of it in which the mixing time is

$$\tau_m = NT_R - t_1$$

Proper combination of the signals from the two experiments yields two-dimensional spectra with pure absorptive line shapes. This modification of the experiment turns out to be essential for the quantitative analysis of such spectra, in particular for cases in which the isotropic shifts of several of the carbon atoms of interest are barely resolved such as tropolone or bullvalene, experiments on which are described in the accompanying paper.[17] All spectra reported in these two papers were recorded by using this modified method.

This rotor-synchronized two-dimensional exchange experiment has been used previously only to study systems characterized by pure reorientation such as dimethylsulfone or poly(oxymethylene).[10-12] In order to apply the method to tropolone (or bullvalene) the situation in which molecular reorientation may be coupled to chemical transformation must be considered. In contrast to the pure reorientation case for which only cross peaks linking different sidebands of the same carbon resonance appear, when chemical transformation takes place cross peaks linking the sidebands of the exchanging atoms are obtained. An analysis of the two-dimensional pattern can provide information about both the geometry and the rate of the reaction and in the present work we present an analysis along these lines for the case of solid tropolone. We find that several different processes occur simultaneously, involving pure reorientation of the molecules as well as a hydrogen shift coupled with reorientation. We propose that all these processes are related to self-diffusion, which is assumed to proceed via random molecular jumps between different sites in the crystal. If crystallographic order is to be preserved, some of the jumps must also be accompanied by a hydrogen shift and/or a molecular reorientation. The hydrogen shift process observed by Maciel and co-workers[6,7] in solid tropolone is therefore merely a consequence of the more fundamental process of molecular self-diffusion. In fact, our model allows an estimate of the diffusion constant in solid tropolone to be made from the rate of the hydrogen shift reaction.

## Experimental Section

Carbon-13 MAS NMR spectra were recorded on a Bruker MSL spectrometer at a frequency of 75.47 MHz. The two-dimensional exchange spectra were obtained by using the sequence shown in Figure 2. In this experiment, cross polarization is triggered by an optical signal reflected from the rotor and is followed by an incremented evolution period, $t_1$. A $\pi/2$ carbon-13 pulse is then applied, which stores the magnetization along the $z$-axis for an approximately preset mixing time. After this, a second optical pulse triggers a short additional delay—of duration equal to the sum of the cross-polarization time and the evolution period for the normal experiment or simply the cross-polarization time for the time-reversed experiment—before the detection pulse. This procedure ensures that the mixing periods in the two experiments are $NT_R$ or $NT_R - t_1$, respectively. The relevant experimental parameters are given in the figure captions. In practice, four experiments are performed in which the real (cosine) and imaginary (sine) components of the magnetization after the evolution period are selected by appropriate phase cycling in both the normal and time-reversed experiments. These are then Fourier transformed and combined as described by Hagemayer et al.[12] in order to obtain spectra with pure absorptive line shapes.

Tropolone was commercially available from Fluka and used without further treatment except that in order to shorten the longitudinal relaxation times the sample was irradiated by electrons with a total dose of 750 kGy. Even then, however, a recycle delay of ~25 s was necessary.

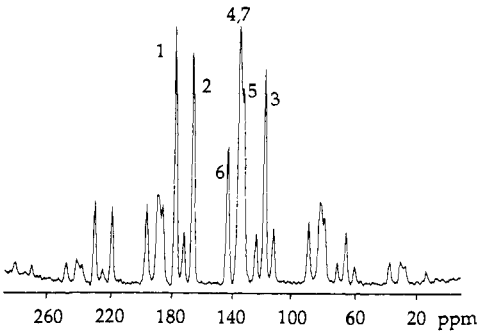


**Figure 3.** One-dimensional carbon-13 CPMAS NMR spectrum of tropolone recorded at 75.47 MHz, rotor frequency 4.2 kHz, and temperature 25 °C. The experimental parameters used were CP contact time 5 ms, recycle time 23 s, and proton pulse length 3.5 μs. The carbon assignment is indicated on the corresponding center peaks.

**Table I.** Chemical Shift Tensors of the Carbon Atoms of Tropolone[a]

| carbon no. | $\sigma_{xx} - \sigma_{zz}$, ppm | $\sigma_{zz}$, ppm[b] | $\sigma_{yy}$, ppm[b] | $\sigma_{xx}$, ppm[b] | $\sigma_{iso}$, ppm[c] |
|---|---|---|---|---|---|
| 1 | 155 | −90 | 25 | 65 | 178.1 |
| 2 | 165 | −90 | 10 | 75 | 166.2 |
| 3 | 166 | −83 | 0 | 83 | 116.5 |
| 4, 7[d] | 200 | −100 | 0 | 100 | 134.0 |
| 5 | 200 | −100 | 0 | 100 | 131.0 |
| 6 | 220 | −110 | 0 | 110 | 142.6 |

[a] Derived from CPMAS spectra by using the Herzfeld–Berger analysis.[20] [b] Relative to the corresponding $\sigma_{iso}$. Estimated accuracy ±10 ppm. [c] Relative to TMS. [d] Peaks due to carbons 4 and 7 are not resolved.

## One-Dimensional Carbon-13 MAS Spectra

A one-dimensional carbon-13 CPMAS NMR spectrum of tropolone with a rotor frequency of 4.2 kHz is shown in Figure 3 together with the peak assignment as proposed by Mori et al.[18] The Herzfeld–Berger analysis[19] was used to derive approximate values for the principal components of the corresponding tensors from this spectrum and several others recorded with lower spinning frequencies. Average results are summarized in Table I, together with the corresponding values for the isotropic chemical shifts. The results for the anisotropic chemical shifts are not very accurate due to the difficulty of determining exact peak intensities, particularly in the presence of a high degree of overlap between lines. However, the results are in general agreement with literature data for similar types of carbon atoms.[20] Note that the values for the principal components of the oxygen-bonded carbon atoms are quite similar and likewise those for the olefinic carbons. Although the sideband intensity analysis does not provide information about the directions of the principal axes of the chemical shift tensor, it can safely be assumed that the most shielded component $\sigma_{zz}$

(17) Titman, J. J.; Luz, Z.; Spiess, H. W. *J. Am. Chem. Soc.*, following paper in this issue.

(18) (a) Mori, A.; Sugiyana, S.; Manetsuka, H.; Tomiyasu, K.; Takeshita, H. *Bull. Chem. Soc. Jpn.* **1987**, *60*, 4339. (b) Masamune, S.; Kemp-Jones, A. V.; Green, J.; Rabenstein, D. L.; Yasunami, M.; Takase, K.; Nozoe, T. *Chem. Soc. Chem. Commun.* **1971**, 360.

(19) Herzfeld, J.; Berger, A. E. *J. Chem. Phys.* **1980**, *73*, 6021.

(20) Veeman, W. S. *Prog. Nucl. Magn. Reson. Spectrosc.* **1984**, *16*, 193.

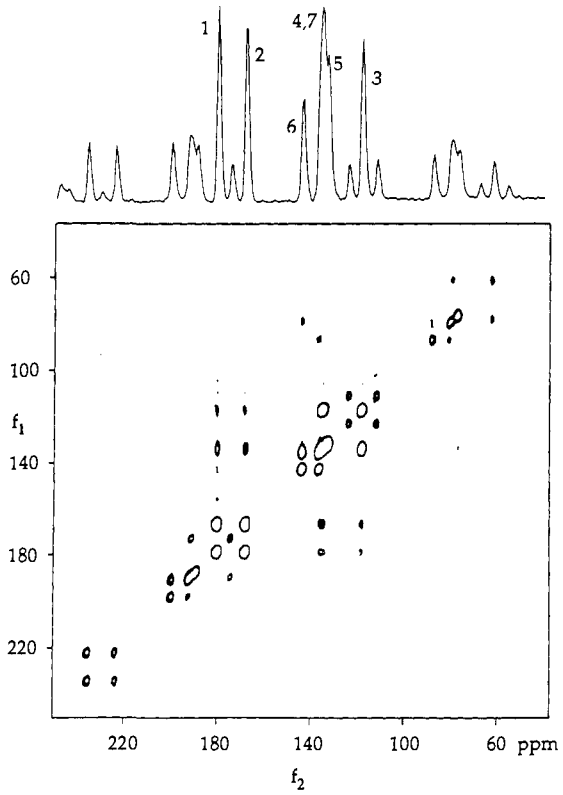


**Figure 4.** Two-dimensional carbon-13 MAS exchange spectrum of tropolone recorded at 40 °C with a rotor-synchronized mixing time of 6 s. The other parameters used were CP contact time 5 ms, recycle time 23 s, rotor frequency 4.2 kHz, and proton and carbon-13 $\pi/2$ pulse lengths 3.5 μs. Eighty $t_1$ increments were used with a maximum $t_1$ value of 3.2 ms. Data acquisition in $t_2$ lasted 10.2 ms. The spectral width in both dimensions was 25000 Hz. Six contours are drawn equally spaced between 50 and 7.5% of the largest peak. There was no intensity at the equivalent negative levels in this spectrum. A one-dimensional CPMAS spectrum with peak assignment on the center bands, recorded with the same parameters, is shown at the top of the diagram. Note, in addition to exchange cross peaks, those linking the center bands of the nonexchanging carbon atoms (4,7 and 3 with 1 and 2) due to spin diffusion.

is directed along the perpendicular to the molecular plane for all atoms.

### Assignment of Carbon-13 Rotor-Synchronized Two-Dimensional MAS Exchange Spectra

Before presenting two-dimensional exchange spectra of tropolone, the question of which cross peaks are expected for the simple hydrogen shift/molecular $\pi$-flip mechanism proposed by Maciel and co-workers[7] will be discussed. Here, a distinction is made between the pairs of carbon atoms that undergo exchange under the effect of the hydrogen shift, (1,2), (3,7), and (4,6), and carbon 5, which retains its chemical identity during this process. In the following discussion, a sideband of order $N$ is defined as that sideband which is shifted by $N\omega_R$ from the center band ($N = 0$) along the positive frequency coordinate and an $n$th order cross peak is the cross peak linking a $N$th order sideband with one of order $N \pm n$. The various cross peaks are classified as "auto" or "hetero" cross peaks according to whether they link different sidebands of the same carbon-13 resonance or sidebands from two chemically different atoms. Note that auto cross peaks occur when the process involves pure reorientation, while hetero cross peaks appear only if there is chemical exchange.

A pure hydrogen shift without a concomitant molecular flip (upper part of Figure 1) interchanges the shift tensors of the exchanging carbon atoms, altering their orientation in the process, while the chemical shift tensor of carbon 5 undergoes an effective reorientation. In the rotor-synchronized two-dimensional exchange spectrum, a pure hydrogen shift will therefore lead to hetero cross peaks linking the sidebands of the exchanging pairs of carbons as well as to auto cross peaks between different sidebands of carbon

**Table II.** Expected[a] Cross Peaks between Carbon-13 Spinning Sidebands in the Two-Dimensional Exchange Spectra of Tropolone for Various Processes in the Solid State

| description of dynamic process | exchanging carbons[b] hetero peaks[c] | exchanging carbons[b] auto peaks[d] | carbon 5 auto peaks | rate constant |
|---|---|---|---|---|
| 1. pure hydrogen shift | + | − | + | |
| 2. hydrogen shift coupled with a molecular $\pi$-flip | + | − | − | $k_1$ |
| 3. diffusive jumps between equivalent dimers | − | − | − | $k_0$ |
| 4. diffusive jumps between inequivalent dimers plus a $\pi$-flip | − | + | + | $k_2$ |
| 5. diffusive jumps between inequivalent dimers plus a hydrogen shift | + | − | + | $k_3$ |

[a] + signs indicate expected cross peaks, − signs those that are not expected. [b] Carbons exchanged by the hydrogen-shift process. [c] Linking pairwise the spinning sidebands of (1,2), (3,7), and (4,6). [d] Linking sidebands of a single carbon atom 1–4, 6, and 7.

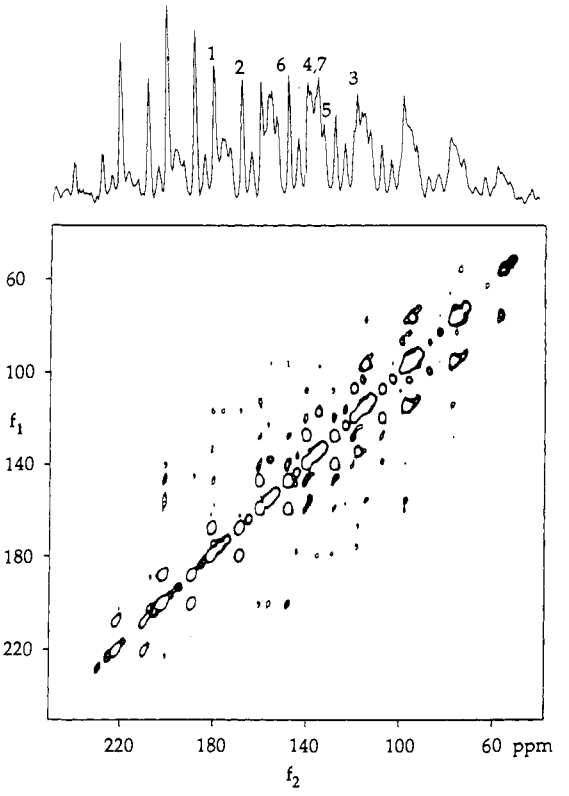


**Figure 5.** Same as in Figure 4 but recorded at a rotor frequency of 1.5 kHz. Note the large number of exchange cross peaks appearing above the noise level in this spectrum.

5. However, no auto cross peaks will be observed for any other carbon atom. This situation is summarized in the first row of Table II. In contrast, if the hydrogen shift involves a concerted molecular flip (second stage in Figure 1), the chemical shift tensor of carbon 5 will remain unchanged, while those of the exchanging carbons will still be affected. Consequently, only hetero cross peaks linking sidebands from the exchanging carbon atoms should be observed but no auto cross peaks for any of the atoms. This situation is depicted in the second row of Table II.

In Figures 4 and 5 are shown carbon-13 two-dimensional exchange spectra of tropolone obtained with the rotor-synchronized sequence of Figure 2 at 40 °C and spinning frequencies of 4.2 and 1.5 Hz, respectively. The parameters used to record these spectra are given in the respective figure captions. The mixing time of 6 s was sufficiently long compared to the reaction half-life[7] of 1.4 s at 40 °C to allow the peak intensities to reach close to

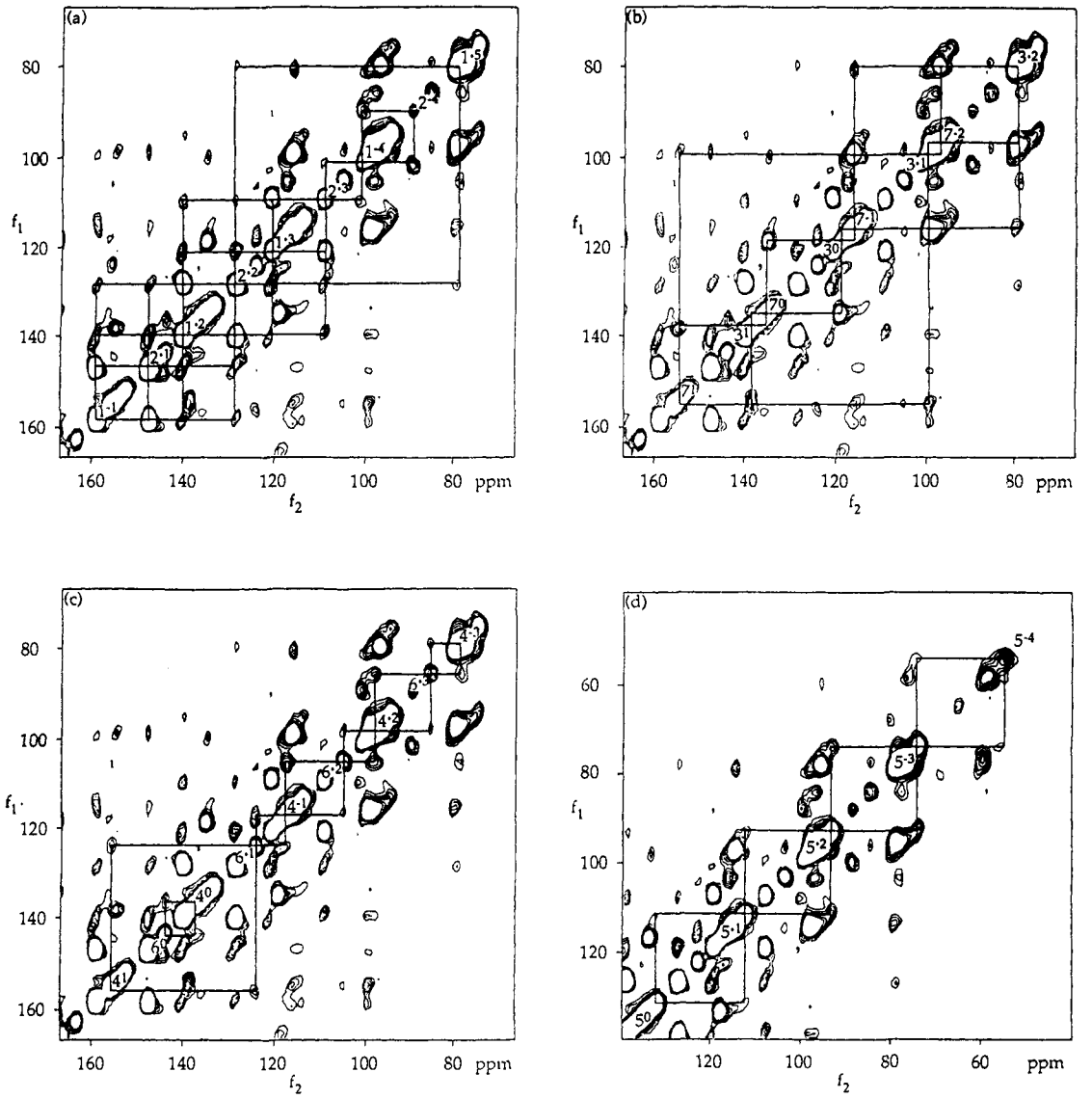


**Figure 6.** Expanded sections of the two-dimensional spectrum of Figure 5 with connectivity networks to facilitate the identification of the various cross peaks. The numbers along the main diagonal identify the carbon atoms and the superscripts the corresponding sideband order $N$. (a) A network linking both hetero and auto cross peaks of carbons 1 and 2. Note the higher order cross peaks such as $I^{2,2}{}_{-2,-3}$ and $I^{1,1}{}_{-1,-2}$ (auto) and $I^{1,2}{}_{-1,-2}$ and $I^{2,1}{}_{-2,-5}$ (hetero), indicating the occurrence of both pure molecular reorientation and hydrogen shift. (b) The same as in (a) for the pair of carbons 3,7. No auto cross peaks are observed in this case. (c) The same but for carbons 4,6. (d) The connectivity lines linking the various sidebands of carbon 5. Such a network indicates that a concerted hydrogen shift/molecular $\pi$-flip mechanism is not the sole dynamic process occurring in solid tropolone.

their asymptotic values. The spectrum obtained at the higher spinning rate (Figure 4) is relatively simple to interprete. It shows hetero cross peaks linking the sidebands of the exchanging carbons but no auto cross peaks linking the sidebands of carbon 5 or of any of the other carbon atoms. On this basis alone, it could be concluded that the hydrogen shift reaction proceeds in concert with a molecular $\pi$-flip as suggested by Maciel and co-workers (second row of Table II). We note, however, that in this spectrum only zero-order hetero cross peaks between the exchanging carbon atoms are clearly observed, although in principle higher order ones are also expected. In fact, the intensities of these higher order cross peaks should be similar to those of the auto cross peaks of carbon 5, which are expected if the hydrogen shift took place without a concerted $\pi$-flip (first row of Table II). Therefore, the absence of the latter cross peaks from the experimental spectrum of Figure 4 cannot be taken as proof for the concerted hydrogen shift/molecular $\pi$-flip mechanism.

Higher order cross peaks are indeed observed in the two-dimensional exchange spectrum of Figure 5, which was recorded at a spinning frequency of 1.5 kHz, nearly a factor of 3 slower than used to record the spectrum of Figure 4. The pattern is now considerably more complicated. The diagonal shows a large number of spinning sidebands ranging from $N = +4$ to $N = -4$ for some of the carbon atoms and many more cross peaks including those of higher order are present. Some of these are indicated in the expanded sections of the 1.5-kHz two-dimensional spectrum in Figure 6. In parts a–d of this figure various cross-peak networks are traced out for each pair of exchanging carbon atoms and for carbon 5. Surprisingly, these networks include auto cross peaks linking different sidebands of carbon 5 (part d) as well as similar auto cross peaks for carbons 1 and 2 (part a). Such cross peaks are not expected to appear if the concerted hydrogen shift/molecular $\pi$-flip mechanism is the sole dynamic process in solid tropolone. In fact, the appearance of auto cross peaks for carbons 1 and 2 indicates the presence of a molecular reorientation process occurring *without* a concomitant hydrogen shift. It must therefore be concluded that at least two dynamic processes occur in solid tropolone: a hydrogen shift reaction (with or without a concomitant molecular $\pi$-flip) and a pure molecular reorientation (without a hydrogen shift). In the next section it is argued that this coexistence of processes can be explained in terms of translational self-diffusion involving molecular jumps between lattice sites in the crystal.

So far the small but visible cross peaks linking the center bands of carbons 4, 7, and 3 with those of carbons 1 and 2 in the spectrum recorded at 4.2 kHz have not been discussed, nor have

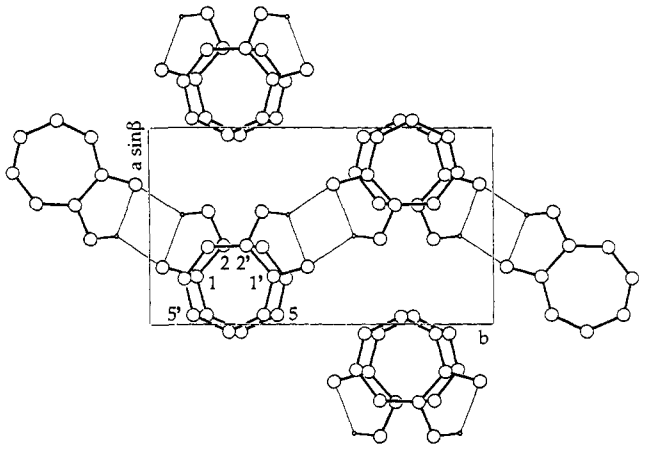


**Figure 7.** Projection of the crystal structure of tropolone on the crystallographic $a^*b$ plane. Note the magnetically inequivalent but symmetry-related hydrogen-bonded dimers in the unit cell. The primed and unprimed numbers refer to the corresponding carbons in the two inequivalent dimers.

similar peaks occurring in the 1.5-kHz spectrum not accounted for by the networks of Figure 6. These peaks can be associated with neither the hydrogen shift nor molecular reorientation because they link carbon atoms not exchanged by the tautomeric reaction. They can, however, be ascribed to spin diffusion. The dynamics of this process between carbon-13 nuclei has been studied by one- and two-dimensional NMR spectroscopy[21] and methods to differentiate it from chemical exchange have been proposed.[22] In general, spin diffusion is only weakly dependent on temperature compared to chemical exchange. The identification of these cross peaks as due to spin diffusion was confirmed by their presence in a similar spectrum recorded at 10 °C, at which temperature the tautomeric process is frozen out and the intense exchange cross peaks disappear.

### Crystal Structure and Diffusional Jumps

The crystal and molecular structure of tropolone was investigated by Shimanouchi and Sasada using X-ray diffractometry.[9] The crystals are monoclinic and belong to the space group $P2_1/c$ with cell dimensions $a = 7.135$, $b = 12.178$, and $c = 7.122$ Å and $\beta = 99.63°$. There are four molecules per unit cell, arranged in two dimers (see Figure 7), which are nearly planar with the planes essentially parallel to the crystallographic $a^*b$ plane. In each dimer, the two monomers are related by a center of symmetry and are therefore magnetically equivalent. The two dimers are related to each other by a glide plane and are in general magnetically inequivalent. Only two distinct molecular sites in the crystal need therefore be considered as indicated, for example, by the primed and unprimed carbon atom numbers in Figure 7.

We propose that the dynamic processes responsible for the cross peaks observed in the two-dimensional carbon-13 exchange spectra of tropolone involve the molecular reorientation and hydrogen shift that may accompany molecular diffusion within the crystal lattice. This translational diffusion most likely proceeds via molecular jumps between different sites induced, for example, by vacancies or other crystal imperfections. A diffusive jump that takes a tropolone molecule from one dimer site into an equivalent one can proceed in two ways without disturbing the crystal order. First, it can undergo pure translation or translation plus a "planar" rotation by 180° (i.e., about an axis perpendicular to the molecular plane). The latter alternative takes the molecule into its centrosymmetric image site in the dimer. Such jumps leave all carbon chemical shift tensors unchanged relative to the crystal lattice and therefore yield no exchange cross peaks in the two-dimensional spectrum. This situation is indicated in the third row of Table II and the corresponding rate constant, which is not measureable from the two-dimensional experiment, is designated $k_0$. Second, the same jump process may involve a molecular $\pi$-flip about an axis in the molecular plane. In this case, it must be accompanied by a hydrogen shift and the situation as far as the NMR spectrum is concerned is the same as for the local concerted hydrogen shift/molecular $\pi$-flip suggested by Maciel and co-workers[6] (Table II, second row). We label the rate constant associated with this process $k_1$.

However, a diffusive jump can also end at a site of a magnetically inequivalent dimer. As may be seen from Figure 7, to preserve crystal order, such a process must be associated with either a molecular $\pi$-flip or with a hydrogen shift. The first possibility corresponds effectively to a planar reorientation and should therefore lead to auto cross peaks for all the tropolone carbon atoms as indicated in the fourth row of Table II. The second possibility corresponds to a hydrogen shift plus reorientation leading to the cross-peak pattern of the fifth row of Table II. We label the rate constants associated with these two possibilities $k_2$ and $k_3$, respectively.

At a sample spinning rate of 1.5 kHz, hetero cross peaks linking the sidebands of exchanging carbons are observed as well as auto cross peaks for carbon 5 and for carbons 1 and 2. None of the isolated mechanisms of Table II is consistent with this result. However, if the diffusional jumps can occur between all sites with or without a concerted $\pi$-flip, all observed peaks can be accounted for. More specifically the fact that auto cross peaks are observed for the exchanging carbons 1 and 2 definitely confirms the occurrence of diffusive jumps between inequivalent sites with $\pi$-flips (line 4 of Table II) since no other mechanism yields such peaks. In principle, auto cross peaks should also occur for the other exchanging carbon atoms but they are apparently too weak to be observed as discussed in the next section. The hetero cross peaks between the exchanging carbon atoms indicate the occurrence of diffusive jumps between equivalent sites with a concerted hydrogen shift/$\pi$-flip (line 2) and/or diffusive jumps between inequivalent sites with a hydrogen shift (line 5). Of course no evidence is provided for the occurrence of simple diffusive jumps between equivalent sites (line 3), but there is no reason to believe that this process does not take place while the others do. The relative importance of the various detectable mechanisms can be obtained from a suitable analysis of the cross-peak intensities. Our results are not sufficient to do so quantitatively and we therefore limit ourselves here to a discussion of the main features of the spectra and a comparison with some theoretical calculations.

### Basic Equations for the Computation of Rotor-Synchronized Two-Dimensional Exchange Spectra

The two-dimensional rotor-synchronized MAS NMR exchange experiment has previously only been considered in connection with pure reorientation processes.[10-12] For the present discussion it is necessary to include the effect of chemical exchange. In the following, therefore, we briefly recapitulate the basic equations necessary for the analysis of the two-dimensional patterns obtained by such experiments with specific application to the case of tropolone.

The time domain signal $S(t_1,t_2;\tau_m)$ obtained from the combined normal and time-reversed rotor-synchronized two-dimensional exchange experiments with the pulse sequence of Figure 2 can in general be written in terms of the sum[12]

$$S(t_1,t_2;\tau_m) = \sum_{i,j} P_{i,j}(\tau_m) S_{i,j}(t_1,t_2) \qquad (1)$$

where $S_{i,j}(t_1,t_2)$ is the contribution from those nuclei that were in site $i$ during the evolution period and in site $j$ during the detection period and $P_{i,j}(\tau_m)$ is the corresponding fractional population. The latter can be obtained from the kinetic equation[15]

$$P_{i,j}(\tau_m) = P_i^0[\exp(\mathbf{K}\tau_m)]_{ij} \qquad (2)$$

where $P_i^0$ is the equilibrium population of site $i$ and $\mathbf{K}$ the exchange matrix. For the case of tropolone we need to distinguish between the exchanging carbon atoms and carbon 5, which can only undergo molecular reorientation. Each of the former can occupy

(21) Reference 15, Chapter 10.
(22) Limbach, H. H.; Wehrle, B.; Schlabach, M.; Kendrick, R.; Yannoni, C. S. *J. Magn. Reson.* **1988**, *77*, 84.

four different sites in the crystal—two sites in each of the two dimers. This is indicated for the case of carbons 1 and 2 by the numbers 1, 2, 1′, and 2′ in Figure 7. Clearly, for these carbon atoms, $P_i^0 = {}^1/_4$ for all sites and in terms of the rate constants defined in Table II

$$\mathbf{K}^{ex} = \begin{bmatrix} -k & k_1 & k_2 & k_3 \\ k_1 & -k & k_3 & k_2 \\ k_2 & k_3 & -k & k_1 \\ k_3 & k_2 & k_1 & -k \end{bmatrix} \tag{3}$$

where the rows and columns are in the order 1, 2, 1′, 2′ and $k = k_1 + k_2 + k_3$. The same exchange matrix holds for other pairs of exchanging carbon atoms. For carbon 5 only two distinct sites need be considered, labeled 5 and 5′ in Figure 7. Accordingly, for this case $P_i^0 = {}^1/_2$ and

$$\mathbf{K}^{rot} = \begin{bmatrix} -k' & k' \\ k' & -k' \end{bmatrix} \tag{4}$$

where $k' = k_2 + k_3$. When the mixing time is long compared with the correlation times, $k_i^{-1}$, of all processes the $P_{i,j}(\tau_m)$'s can be assumed to have reached their asymptotic values, which are ${}^1/_{16}$ for the exchanging pairs of carbons and ${}^1/_4$ for carbon 5. In the following, we shall assume that in our experiments the long mixing time limit has been reached.

In the absence of relaxation effects, the time domain signal, $S_{i,j}(t_1,t_2)$, is given by the following series of equations

$$S_{i,j}(t_1,t_2) = \sum_{M,N} \exp[i(\omega_L \sigma^i_{iso} + M\omega_R)t_1] \exp[i(\omega_L \sigma^j_{iso} + N\omega_R)t_2] F^{ij}_{M,N} \tag{5}$$

where

$$F^{ij}_{M,N} = (4\pi)^{-1} \int d\alpha \int d\beta \sin\beta \{F^i_M\}^* F^j_N F^{ij}_{M-N} \tag{6}$$

$$F^i_M = (2\pi)^{-1} \int d\gamma \exp[-iM\gamma] f^i(\gamma) \tag{7}$$

$$F^{ij}_{M-N} = (2\pi)^{-1} \int d\gamma \exp[-i(M-N)\gamma] f^i(\gamma) \{f^j(\gamma)\}^* \tag{8}$$

and the $f^j(\gamma)$ functions are defined as

$$f^j(\gamma) = \exp[i(A^j \sin 2\gamma - B^j \cos 2\gamma + C^j \sin\gamma - D^j \cos\gamma)] \tag{9}$$

with

$$A^j = \frac{\omega_L}{6\omega_R}\left\{\frac{3}{2}(\sigma^j_{33} - \sigma^j_{iso}) \sin^2\beta - \frac{1}{2}\left[\frac{1}{2}(\sigma^j_{22} - \sigma^j_{11}) \cos 2\alpha - \sigma^j_{12} \sin 2\alpha\right](\cos 2\beta + 3) - [\sigma^j_{13} \cos\alpha + \sigma^j_{23} \sin\alpha] \sin 2\beta\right\}$$

$$B^j = \frac{\omega_L}{3\omega_R}\left\{\left[\frac{1}{2}(\sigma^j_{22} - \sigma^j_{11}) \sin 2\alpha + \sigma^j_{12} \cos 2\alpha\right] \cos\beta + [\sigma^j_{13} \sin\alpha - \sigma^j_{23} \cos\alpha] \sin\beta\right\}$$

$$C^j = \frac{2^{1/2}\omega_L}{3\omega_R}\left\{-\frac{3}{2}(\sigma^j_{33} - \sigma^j_{iso}) \sin 2\beta - \left[\frac{1}{2}(\sigma^j_{22} - \sigma^j_{11}) \cos 2\alpha - \sigma^j_{12} \sin 2\alpha\right] \sin 2\beta + 2[\sigma^j_{13} \cos\alpha + \sigma^j_{23} \sin\alpha] \cos 2\beta\right\}$$

$$D^j = \frac{2(2^{1/2})\omega_L}{3\omega_R}\left\{\left[\frac{1}{2}(\sigma^j_{22} - \sigma^j_{11}) \sin 2\alpha + \sigma^j_{12} \cos 2\alpha\right] \sin\beta - [\sigma^j_{13} \sin\alpha - \sigma^j_{23} \cos\alpha] \cos\beta\right\} \tag{10}$$

In these equations $\sigma^j_{iso}$ is the isotropic chemical shift in site $j$ and the $\sigma^j_{nm}$ ($n, m = 1, 2, 3$) are the components of the anisotropic chemical shift tensors in the molecular frame. This coordinate system is related to the rotor frame by the three Euler angles, $\alpha$ (representing rotation about the molecular 3-axis), $\beta$ (which is the angle between the molecular 3-axis and the rotor principal axis), and $\gamma$ (which represents rotation about the rotor axis).

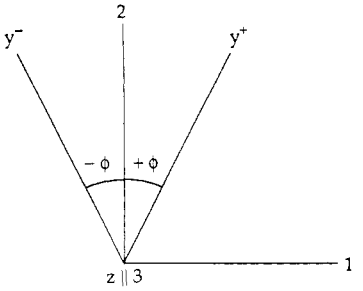


Figure 8. Relation between the chemical shift tensors before and after the reorientation. The axes 1, 2, and 3 are molecular-fixed coordinates with 3 being perpendicular to the molecular plane and 2 bisecting the angle between the $y$ principal axes of the chemical shift tensors before ($y^+$) and after ($y^-$) the reorientation.

For tropolone, because of its nearly planar structure, it is convenient to define the molecular fixed coordinate system 1, 2, 3 with 3 perpendicular to the molecular plane. For symmetry reasons this direction must be a principal axis for all the chemical shift tensors of the tropolone carbon atoms and, as indicated before, it is identified with the most shielded chemical shift tensor component $\sigma_{zz}$ of Table I. The other two principal components lie in the molecular plane but their orientation in the molecule-fixed frame is not known. The chemical shift tensor components are, therefore, expressed in terms of a variable parameter $\phi$ corresponding to the angle between the $y$-axis of the principal chemical shift tensor and axis 2 of the molecular frame (see Figure 8) so that

$$\begin{aligned} \sigma^i_{33} &= \sigma^i_{zz} \\ \sigma^i_{22} &= \sigma^i_{xx} \sin^2\phi^i + \sigma^i_{yy} \cos^2\phi^i \\ \sigma^i_{11} &= \sigma^i_{xx} \cos^2\phi^i + \sigma^i_{yy} \sin^2\phi^i \\ \sigma^i_{12} &= (1/2)(\sigma^i_{yy} - \sigma^i_{xx}) \sin 2\phi^i \\ \sigma^i_{13} &= \sigma^i_{23} = 0 \end{aligned} \tag{11}$$

For each site, an appropriate set of principal chemical shift tensor components $\sigma^i_{\alpha\alpha}$ ($\alpha = x, y, z$) need to be chosen. From Table I, however, the values estimated for the oxygen-bonded carbons 1 and 2 are similar and likewise for the olefinic carbon atoms 3–7. Therefore, we use just two shift tensors for our calculations, corresponding to the rough estimates $\sigma_{xx} = 80$, $\sigma_{yy} = 20$, and $\sigma_{zz} = -100$ ppm for carbons 1 and 2 and $\sigma_{xx} = 80$, $\sigma_{yy} = 0$, and $\sigma_{zz} = -80$ ppm for carbons 3–7. It is then convenient to take the molecular frame axis 2 along the bisector of the $y$ principal axes before and after the jump (see Figure 8), corresponding respectively to $+\phi$ and $-\phi$ in eq 11, so that the overall reorientation angle is $2\phi$. Thus, only two sets of intensities $F^{ij}_{N,M}$ need to be calculated for a given $\phi$, namely, for the oxygen-bonded carbon atoms and for the olefinic carbon atoms, and the numerical results can be applied to both hetero and auto cross peaks. A large simplification of the necessary calculations can be achieved in this fashion.

An approximation for the angles $2\phi^i$ which serves as a guide in the discussion of the results, is to assume that $\sigma_{yy}$, the intermediate principal tensor component, lies along the double bond associated with the corresponding atom in the ground valence state of tropolone. In this approximation, the $2\phi^i$'s for the different diffusion mechanisms of Table II can be estimated from the crystal and molecular structures shown in Figure 7. The results are summarized in Table III. It should be emphasized that the actual values of the reorientation angles may be quite different since neighboring groups and polar resonance structure effects may cause the principal $y$-axes to differ significantly from the directions of the double bonds.

**Table III.** Approximate Change in the Double Bond Direction (in Degrees) for the Various Tropolone Carbons for the Three Jump Diffusion Mechanisms of Table II

| | carbon | | | | | | |
|---|---|---|---|---|---|---|---|
| process[a] | 1 | 2 | 3 | 4 | 5 | 6 | 7 |
| 2 | 13 | 13 | 23 | 77 | 0 | 77 | 23 |
| 4 | 31 | 5 | 5 | 26 | 26 | 52 | 52 |
| 5 | 18 | 18 | 28 | 52 | 26 | 52 | 28 |

[a] Numbers refer to the corresponding lines in Table II.

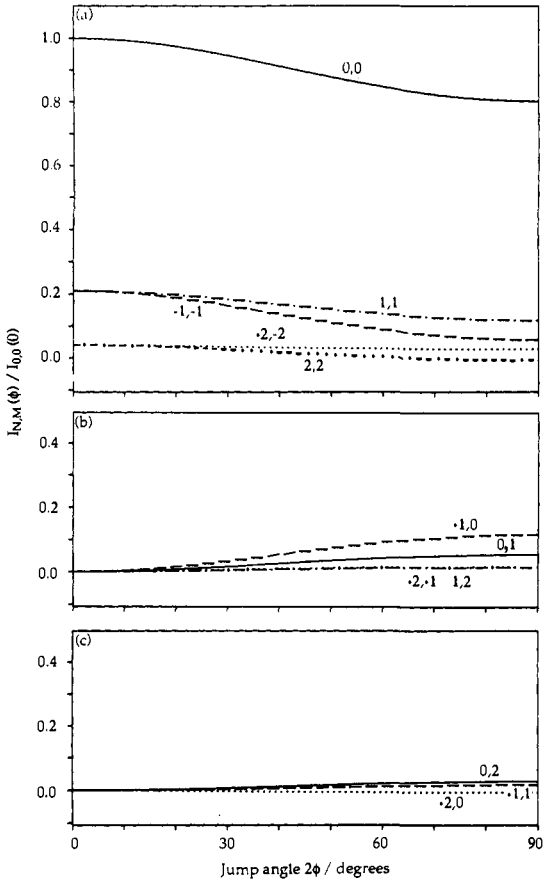


**Figure 9.** Cross-peak intensities $I_{N,M}(\phi)$ of order $|N - M|$ equal to 0 (a), 1 (b), and 2 (c) for the values of $N$ and $M$ indicated as a function of the reorientation angle $2\phi$ defined in Figure 8. The calculations are for a sample spinning frequency of 4.2 kHz, a Larmor frequency of 75.47 MHz, and the set of chemical shift parameters (both before and after the jump) of $\sigma_{xx} = 80$, $\sigma_{yy} = 0$, and $\sigma_{zz} = -80$ ppm, corresponding approximately to the olefinic carbons of tropolone. The intensities are normalized with respect to $I_{0,0}(0)$.

## Results of the Computation and Comparison with Experiments

Under the assumptions outlined in the previous section, eq 10 is much simplified and becomes

$$A^{\pm} = \frac{\omega_L}{12\omega_R}\Big[3(\sigma_{zz} - \sigma_{iso}) \sin^2 \beta - \frac{1}{2}(\sigma_{yy} - \sigma_{xx}) \cos (2\alpha \pm 2\phi)(\cos 2\beta + 3)\Big]$$

$$B^{\pm} = \frac{\omega_L}{6\omega_R}[(\sigma_{yy} - \sigma_{xx}) \sin (2\alpha \pm 2\phi) \cos \beta]$$

$$C^{\pm} = \frac{2^{1/2}\omega_L}{6\omega_R}[-3(\sigma_{zz} - \sigma_{iso}) \sin 2\beta - (\sigma_{yy} - \sigma_{xx}) \cos (2\alpha \pm 2\phi) \sin 2\beta]$$

$$D^{\pm} = \frac{2^{1/2}\omega_L}{3\omega_R}[(\sigma_{yy} - \sigma_{xx}) \sin (2\alpha \pm 2\phi) \sin \beta] \qquad (12)$$

where the ± signs refer to the $f(\gamma)$ functions before (+) and after

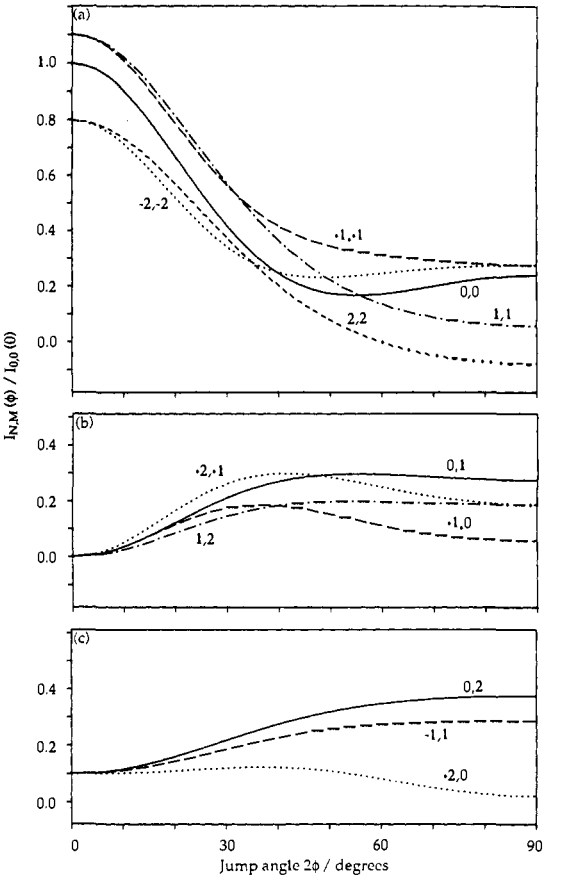


**Figure 10.** Same as Figure 9 but for a sample spinning frequency of 1.5 kHz.

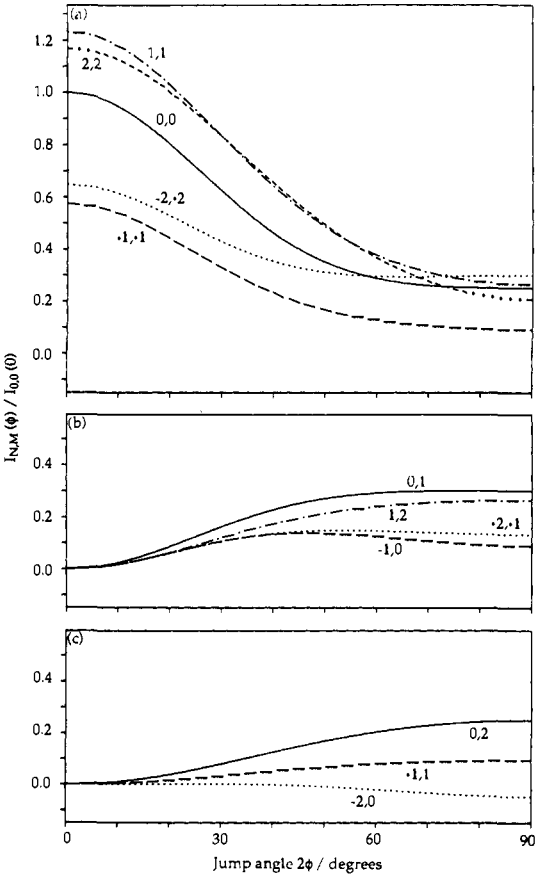


**Figure 11.** Similar plots as in Figure 10 but for a chemical shift tensor $\sigma_{xx} = 80$, $\sigma_{yy} = 20$, and $\sigma_{zz} = -100$ ppm, corresponding approximately to the carbonyl and hydroxyl carbon atoms of tropolone.

(-) the reorientation and the chemical shift tensor components are given in the principal axes system. It can be seen from eq 12 that the cross-peak intensities and their $\phi$-dependence are a function of $|\sigma_{yy} - \sigma_{xx}|$, which is the only part of the tensor modulated by the planar reorientation process discussed here. For the tropolone carbon atoms $|\sigma_{yy} - \sigma_{xx}|$ spans only a fraction of the overall chemical shift anisotropy. Consequently, only weak higher order cross peaks can be expected and then only at low spinning rates, as observed experimentally.

Figures 9–11 show plots of calculated cross-peak intensities of order 0, 1, and 2 for the two sets of chemical shift parameters discussed above and spinning frequencies of 1.5 and 4.2 kHz. All intensities are normalized with respect to $I^{ij}_{0,0}$ at $\phi = 0$. The plots are symmetric about $2\phi = 90°$ because a planar jump of $2\phi = \pi/2 + \epsilon$ has the same effect as a jump of $2\phi = \pi/2 - \epsilon$. Therefore, only plots for $2\phi$ between 0 and $\pi/2$ are shown.

The most conspicuous cross peaks in the spectra under consideration are those of zero order (plots a in Figures 9–11). For our dynamic model, planar reorientation about a principal direction ($z$) of the chemical shift tensor, the expression for their intensities acquires a relatively simple form

$$I_{N,N}(\phi) = (4\pi)^{-1} \int d\alpha \int d\beta \sin\beta \, |F_M|^2 G(\phi) \qquad (13)$$

where

$$G(\phi) = (2\pi)^{-1} \int d\gamma \exp\left\{ i \left[ \frac{\omega_L}{3\omega_R} (\sigma_{yy} - r_{xx}) \sin 2\phi \right] \times \right.$$
$$\left[ \frac{1}{4} \sin 2\alpha \, (\cos 2\beta + 3) \sin 2\gamma - \cos 2\alpha \cos\beta \cos 2\gamma + \right.$$
$$\left. \left. 2^{1/2} \sin 2\alpha \sin 2\beta \sin\gamma - 2(2^{1/2}) \cos 2\alpha \sin\beta \cos\gamma \right] \right\} \qquad (14)$$

In fact, for small $\phi$, the zero-order cross peaks are always the dominant ones in the two-dimensional spectrum, and for $\phi = 0$, under the assumptions above their intensities are identical with those given by the Herzfeld–Berger analysis for the spinning sidebands of corresponding order. With increasing $\omega_R$, their intensity gradually decreases except for $I_{0,0}$, which becomes the dominant cross peak in the spectrum. However, the sensitivity of its intensity to the reorientation angle decreases (see Figures 9 and 10). This reflects the fact that two-dimensional exchange spectra obtained at very high spinning speeds are not very useful for determining geometries associated with a dynamic process, although they are very convenient for extracting kinetic parameters as in the liquid state. In fact, the original two-dimensional spectra of Maciel and co-workers[6,7] were recorded in this limit.

At lower spinning frequencies, on the other hand, the zero-order cross peaks are useful for the determination of reorientation angles. Referring to the experimental results of Figures 4–6, it can be seen that, while at 4.2 kHz the zero-order cross peaks for all the carbon atoms are fairly intense and comparable to the corresponding diagonal peaks, at 1.5 kHz the different pairs of exchanging carbon atoms show different characteristics. Thus, while carbons 1 and 2 exhibit intense zero-order cross peaks for all sidebands with $N = -3$ to 2, the corresponding cross peaks for the pair of carbons 4 and 6 are much weaker, having similar intensities to the higher order cross peaks. For these latter carbons, zero-order cross peaks are only observed for $N = -3$ to 0. The calculated intensities for 1.5 kHz (Figures 10a and 11a) show that as $2\phi$ becomes large the intensity of the zero-order cross peaks for $N > 0$ decreases faster than that for $N < 0$. In addition to this, at large $2\phi$, the intensities of the zero-order cross peaks are comparable with those of the first-order ones. Comparison with the experimental results suggests the conclusion that for carbons 1 and 2 $2\phi < 30°$ while for carbons 4 and 6 $2\phi > 50°$ with carbons 3 and 7 occupying an intermediate position. These estimates for the reorientation angle tie in well with the crude estimates for the various jump mechanisms in Table III.

Such considerations demonstrate the potential usefulness that the zero-order cross peaks may have in determining geometric parameters associated with dynamic processes if accurate values for their intensities can be determined. The relative intensities of the different zero-order cross peaks, their intensities relative to those of higher order ($n > 0$) peaks, and their behavior at different spinning speeds are all a sensitive guide to the reorientation angle. Studies at different sample spinning rates are, therefore, particularly helpful. It should be noted, however, that the zero-order cross peaks can only be measured for processes involving chemical exchange between carbons with different isotropic chemical shifts. For pure reorientation where there is no change in the isotropic shift, these auto cross peaks fall on top of the corresponding diagonal peaks and there intensities are not measureable.

For large reorientation angles or low spinning frequencies, the intensities of the zero-order peaks reduce considerably and may even become negative. In this region the higher order cross peaks are more intense. These higher order peaks always vanish at $2\phi = 0$ under the assumptions made above and they are very small for $2\phi$ less than 20° or so. However, above this value some of their intensities become significant and they provide a useful tool for determining the geometries associated with dynamic processes. A comparison of Figures 10b and 11b shows the sharp dependence of the relative intensities of, for example, the first-order peaks on both the reorientation angle and the components of the shift tensor. In connection with this, note the first-order hetero cross peaks (with $M = -1$ and $N = 0$) linking carbons 4 and 6 in the 4.2-kHz spectrum of Figure 4 (only the cross peaks on the upper left side of the diagonal are observed). Comparison with the calculations for Figure 9 shows that indeed of the plotted higher order cross peaks this is precisely the one reaching an intensity higher than 10% of the center band at $2\phi = 0$ and then only for $2\phi$ larger than 50°. As mentioned above, our data do not allow a full quantitative analysis of the cross-peak intensities, but this example may serve to illustrate the potential power of such an analysis. In the present work, the very identification of higher order peaks, in particular the auto cross peaks for carbons 1, 2, and 5, has been crucial in the interpretation of the experimental results in terms of the diffusive jump model. A quantitative analysis of the results would also allow us to determine the relative weights of the various jump processes in Table II (except of course $k_0$).

It should be emphasized that part of the above discussion applies specifically to the particular chemical shift tensors and geometrical parameters considered here for tropolone but need not be generally true. For instance the vanishing of higher order cross peaks for $2\phi = 0$ is only true if the components of the chemical shift tensor before and after the dynamic process are identical (see eqs 6–8).

## Summary and Conclusions

The cross-peak patterns obtained in the carbon-13 MAS rotor-synchronized two-dimensional exchange spectra of solid tropolone show the presence of at least two distinct dynamic processes involving respectively a hydrogen shift coupled with molecular reorientation and a pure molecular reorientation. Both processes can be accounted for in terms of self-diffusion mechanisms proceeding via molecular jumps between different lattice sites. To preserve crystal order, the jumps connecting inequivalent sites must be accompanied by either a hydrogen shift or a molecular flip, while jumps between equivalent sites may involve both in a concerted fashion. The sum of all the processes leads to the complicated cross-peak pattern observed experimentally. Values for the reorientation angle $2\phi^i$ derived from a comparison of observed cross-peak intensities with calculated ones are in good agreement with those estimated for the different model mechanisms from the crystal and molecular structure of tropolone. The relation between the hydrogen shift and the diffusive jumps allows an estimate to be made of the self-diffusion in tropolone. Assuming similar rate constants for the various mechanisms in Table II, we may define an overall jump rate $k_J = 2(k_1 + k_3)$. To determine the self-diffusion constant we use Einstein's diffusion equation

$$l^2 = 6Dt$$

and identify $l$ with an average distance between lattice sites and

$t$ with the mean lifetime between jumps ($k_J^{-1}$). Taking $l \cong 5$ Å and $k_J \cong 0.2\ s^{-1}$ at room temperature gives $D \cong 4 \times 10^{-21}\ m^2\ s^{-1}$. This result is comparable with that obtained for some other compounds with similar molecular sizes.[23,24] For example, for naphthalene at room temperature $D \cong 2.5 \times 10^{-20}\ m^2\ s^{-1}$. The high activation energy determined by Maciel and co-workers[7] for the tautomeric shift reaction must therefore be ascribed to the self-diffusion process associated with the hydrogen shift (Table II).

Rotor-synchronized two-dimensional MAS exchange spectroscopy may prove useful in other solid systems where coupling between translational diffusion, chemical exchange, and molecular reorientation are involved. When the two-dimensional method is applicable, the difficulties associated with single-crystal work can be circumvented. In the following paper,[17] we describe similar investigations on solid bullvalene for which the tautomeric bond shift reaction (the Cope rearrangement) in the solid state is coupled to a molecular reorientation process. In this case, the mixing time dependence of the cross-peak intensities has been used to estimate the reaction rates and to test mechanistic proposals.

**Acknowledgment.** We thank Dr. B. Blümich for his help and interest in this research. J.J.T. thanks the Science and Engineering Research Council of Great Britain for a NATO Fellowship and Z.L. thanks the Minverva Foundation for a visiting scientist fellowship.

**Registry No.** Tropolone, 533-75-5.

(23) Sherwood, J. N. *Mol. Cryst. Liq. Cryst.* **1969**, *9*, 37.
(24) Resing, H. A. *Mol. Cryst. Liq. Cryst.* **1969**, *9*, 101.

# Solid-State Reactions Studied by Carbon-13 Rotor-Synchronized Magic Angle Spinning Two-Dimensional Exchange NMR. 2. The Cope Rearrangement and Molecular Reorientation in Bullvalene

**Jeremy J. Titman, Zeev Luz,† and Hans W. Spiess***

*Contribution from the Max-Planck-Institut für Polymerforschung, Postfach 3148, D-6500 Mainz, Germany.* *Received November 12, 1991*

**Abstract:** Carbon-13 MAS NMR measurements are reported for solid bullvalene between −40 and +85 °C. One-dimensional spectra recorded above −10 °C exhibit, as a function of increasing temperature, dynamic line broadening, followed by coalescence and, eventually, narrowing. Analysis of the line widths in the slow exchange regime indicates the presence of two independent dynamic processes: symmetric threefold jumps and bond shift tautomerism (the Cope rearrangement). Two-dimensional exchange experiments with rotor-synchronized mixing times are presented in the temperature range −20 to −10 °C with mixing times of 4–500 ms. These experiments were carried out at a slow spinning rate for which auto cross peaks between the olefinic carbon atoms as well as hetero cross peaks between the latter and the aliphatic carbons are observed. The results of these experiments are consistent with the occurrence of the two processes determined by the one-dimensional experiments and by earlier deuterium measurements and confirm that the Cope rearrangement proceeds in concert with a molecular reorientation process that preserves the crystal ordering. The estimated activation energies for the threefold jumps and the concerted Cope rearrangement/reorientation are found to be approximately 21 and 15 kcal mol$^{-1}$, respectively.

## Introduction

Bullvalene provides a unique example of the Cope rearrangement reaction. Due to the high symmetry of the molecule, more than one million (10!/3) degenerate tautomeric isomers interconvert by this process.[1] Extensive measurements of the kinetics

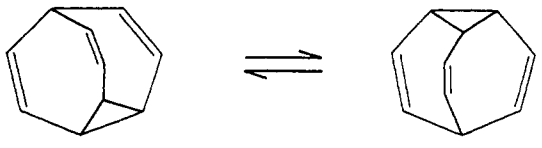

of the reaction in solution have been performed[2-6] since the first synthesis of bullvalene in 1963.[7] For many years it was thought that the Cope rearrangement could not take place in solid bullvalene since the process would perturb the crystal structure, known from X-ray and neutron diffraction to be highly ordered.[8,9] A sharp dispersion in the proton NMR second moment that occurs in solid bullvalene at around room temperature[10] was, therefore, interpreted in terms of the onset of symmetric threefold jumps of the molecules, a process that does not affect the crystal order. In 1985, however, Meier and Earl[11] showed, using carbon-13 magic angle spinning (MAS) NMR, that the observed dispersion must be due at least in part to the Cope rearrangement. They found that the resolved resonances observed for the aliphatic and olefinic carbon nuclei at low temperatures (−60 °C) coalesce and merge to a single line above room temperature. This effect can only be

† Permanent address: The Weizmann Institute of Science, Rehovot 76100, Israel.

(1) Doering, W. von E.; Roth, W. R. *Tetrahedron* **1963**, *19*, 715.
(2) (a) Saunders, M. *Tetrahedron Lett.* **1963**, *25*, 1699; (b) *Magnetic Resonance in Biological Systems*; Pergammon Press: New York, 1967; p 85.
(3) Oth, J. F. M.; Mullen, K.; Gilles, J.-M.; Schröder, G. *Helv. Chim. Acta* **1974**, *57*, 1415.
(4) (a) Gunther, H.; Ulmen, J. *Tetrahedron* **1974**, *30*, 3781. (b) Nakanishi, H.; Yamamoto, O. *Tetrahedron Lett.* **1974**, *20*, 1803. (c) Additional references in isotropic solutions of bullvalene may be found in: Mann, B. E. *Prog. Nucl. Magn. Reson. Spectrosc.* **1977**, *11*, 95.
(5) Huang, Y.; Macura, S.; Ernst, R. R. *J. Am. Chem. Soc.* **1981**, *103*, 5327.
(6) (a) Poupko, R.; Zimmermann, H.; Luz, Z. *J. Am. Chem. Soc.* **1984**, *106*, 5391. (b) Boeffel, C.; Poupko, R.; Zimmermann, H.; Luz, Z. *J. Magn. Reson.* **1989**, *85*, 329.
(7) Schröder, G. *Angew. Chem., Int. Ed. Engl.* **1963**, *2*, 481.
(8) (a) Johnson, S. M.; McKechnie, J. S.; Lin, B. T.-S.; Paul, I. C. *J. Am. Chem. Soc.* **1967**, *89*, 7123. (b) Amit, A.; Huber, R.; Hoppe, W. *Acta Crystallogr.* **1968**, *B24*, 865.
(9) (a) Luger, P.; Buschmann, J.; McMullan, R. K.; Rube, J. R.; Matias, P.; Jeffrey, G. A. *J. Am. Chem. Soc.* **1986**, *108*, 7825. (b) Luger, P.; Buschmann, J.; Richter, T.; McMullan, R. K.; Ruble, J. R.; Matias, P.; Jeffrey, G. A. *Acta Crystallogr.* **1987**, *A43*, C-105.
(10) Graham, J. D.; Santee, E. R., Jr. *J. Am. Chem. Soc.* **1966**, *88*, 3453.
(11) Meier, B. H.; Earl, W. L. *J. Am. Chem. Soc.* **1985**, *107*, 5553.

0002-7863/92/1514-3765$03.00/0 